PCCP

Cite this: *Phys. Chem. Chem. Phys.*, 2012, **14**, 5052–5062

www.rsc.org/pccp

PERSPECTIVE

Ionic liquids in confined geometries

Susan Perkin

Received 30th November 2011, Accepted 12th January 2012
DOI: 10.1039/c2cp23814d

Over recent years the Surface Force Apparatus (SFA) has been used to carry out model experiments revealing structural and dynamic properties of ionic liquids confined to thin films. Understanding characteristics such as confinement induced ion layering and lubrication is of primary importance to many applications of ionic liquids, from energy devices to nanoparticle dispersion. This Perspective surveys and compares SFA results from several laboratories as well as simulations and other model experiments. A coherent picture is beginning to emerge of ionic liquids as nano-structured in pores and thin films, and possessing complex dynamic properties. The article covers structure, dynamics, and colloidal forces in confined ionic liquids; ionic liquids are revealed as a class of liquids with unique and useful confinement properties and pertinent future directions of research are highlighted.

1. Introduction

Many emerging applications of ionic liquids (ILs) rely upon their confinement into narrow pores or thin films. These applications can be divided into three main classes: ILs as electrolytes in energy devices;[1–4] ILs as lubricants or surface modifiers;[5–7] and ILs as solvents for nanoparticle dispersion and colloidal materials.[8,9] Examples of recent IL technologies include supercapacitors based on IL electrolytes,[2,4] dye-sensitised solar cells,[3] and dispersions of carbon nanotubes in IL for conductive gels[9] and elastic electronics.[8] Despite these technological developments, fundamental aspects of the structure and properties of ILs nano-confined to films or pores have been relatively little studied. This is partly due to the recent emergence of the field and, principally, to the great difficulty of accessing this regime in well-defined model experiments. Questions arising include the following: 'What is the distribution of cations and anions in the vicinity of confining surfaces, and how is it affected by surface charge?', 'What is the mechanism of dissipating shear stress across IL?', and 'How does IL mediate colloidal forces?'. The aim of this Perspective is to provide an overview of the current state of progress in answering these questions and to highlight where more work needs to be done.

We (somewhat arbitrarily) define a liquid as being in a 'confined geometry' when it is bounded by solid walls such that the molecular dimension of the liquid is within a factor of 10 of the smallest dimension of the confining structure. Typically this involves an IL ion size of order $\sim$ 1 nm and a pore width or film thickness of $\leq$ 10 nm. In such systems a large fraction of the molecules (or ions) are in close proximity to the confining walls and in many cases this causes the liquid structure and interactions to be perturbed relative to their bulk values.

The confinement of (non-ionic) liquids to such geometries can have dramatic effects on the physical properties of the liquid; it cannot be assumed that bulk characteristics such as viscosity or conductivity will remain unchanged for a confined liquid. For example non-polar liquids such as cyclohexane or toluene can undergo a spontaneous phase change from liquid to solid when squeezed between solid walls into films thinner than approximately 5–10 molecular diameters.[10,11] On the other hand, pure water and electrolyte solutions confined to similar and even thinner films retain their bulk-like fluidity even under high external pressure.[12–14] Confinement of ionic liquids into pores or films might be expected to alter the structure, dynamic properties, and the mediation of forces and fields: each of these factors should be understood in order to take full advantage of the unique range of properties of ILs compared to conventional solvents (Fig. 1). For example, dispersion of carbon nanotubes and metal nanoparticles relies upon fine tuning of colloidal interactions in the IL medium; and use of ILs as supercapacitor electrolytes requires rapid dynamic relaxation of the IL when the electrode voltage is changed. This Perspective inspects and compares results from recent experimental and simulation studies of IL in well-defined confined geometries. Whilst there are many interesting questions relating to the properties of ILs near isolated surfaces—such as the structure of the 'electrical double layer' and the orientation of ions in the first layer—we restrict ourselves here to those which apply specifically to IL confined in space by more than one wall so that at least one dimension of the system is on the molecular or nanoscopic scale. This includes the film of liquid between two interacting colloidal particles, which can comprise two *overlapping* electrical double layers. We consider in turn the effect of confinement on

Department of Chemistry, University College London, WC1H 0AJ, London, UK. E-mail: susan.perkin@ucl.ac.uk

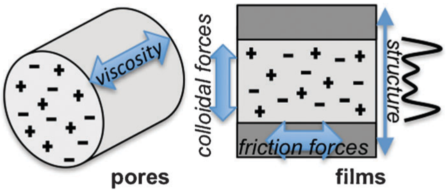

Fig. 1 Ionic liquids in confined geometries are studied in model experiments using either pores (left) or thin films (right). In this Perspective we discuss and compare experiments studying the effect of confinement on liquid structure, dynamics including viscosity and lubrication, and colloidal forces.

structure (Section 2), dynamics (Section 3), and the mediation of colloidal forces and nanoparticle stabilisation (Section 4). Section 5 provides a summary and outlook.

2. Structure of confined ionic liquids

2.1. From bulk to the interface to confinement

We cannot sensibly consider the structure of ILs in confined geometries without first knowing something about their liquid structure in the bulk (away from any interfaces) and adjacent to a single solid surface. Although not the focus of this Perspective, we begin this section by directing the reader to sources of information about these topics. Molecular organisation in bulk ILs is, at least in some cases, far from homogeneous: it has been shown in both experiment and simulations that nano-scale ordering arises from the association of polar and non-polar moieties[15–20] (see also the *Phys. Chem. Chem. Phys.* themed issue on 'Nanostructure in ionic liquids'[21]). Where ionic liquid meets a surface, additional structuring influences arise from the steric constraints and field effects at the interface. This has been shown to lead, for some ILs, to alternating layers of cations and anions at an isolated (negatively charged) sapphire surface;[22] but not for others.[23] Simulations where the ions were represented by hard-spheres showed similar alternation of cations and anions.[24,25] Atomistic molecular dynamics simulations also demonstrated molecular layering in the IL adjacent to a single interface:[26–30] ions are distributed into layers, typically three distinct layers being apparent before the liquid structure is indistinguishable from the bulk, and alternation of cations and anions was observed in response to an imposed surface charge.[29,30] AFM experiments in Atkin's group have shown how the ion layering structure in IL adjacent to a solid surface depends on surface chemistry,[31] temperature,[32] surface charge,[33] and ion type.[34] Importantly, these experiments and simulations invariably show that the electrical double layer (EDL)—for these purposes defined as the region of the liquid perturbed by an adjacent charged surface—is much larger than a single ion layer thick. This demonstrates the inadequacy of classical Poisson–Boltzmann based theories to explain screening effects in ILs: the EDL in IL is at least an order of magnitude larger than predicted by calculation of a Debye screening length. The fundamentally different structure of IL-solid compared to dilute electrolyte-solid interfaces originates in the overscreening effect, arising from ion correlations when the ion concentration is high and the surface charge is relatively low, and the crowding effect which occurs at higher surface charge when one layer of the large ions cannot provide sufficient screening.[24,25,35,36]

2.2. Ionic liquid structure in thin films

Well-defined model experiments of IL confined to thin films have been performed using a Surface Force Apparatus (SFA, also called Surface Force Balance, SFB) in the research groups of Horn,[37] Perkin,[38,39] Kurihara,[40] and Bureau;[41] each concurring that IL is arranged in layers when confined to a film between two atomically-smooth negatively charged surfaces. In these experiments two molecularly smooth and macroscopic solid walls (usually mica) are gradually brought towards one another across a film of the IL. The liquid is in contact with a 'bath' of bulk liquid, and is squeezed out of the film into the bath as the surfaces approach (and *vice versa*); Fig. 2a. The force (and interaction energy) between the surfaces is detected as a function of the surface separation (*i.e.* film thickness), D, using white light interferometry to measure the film thickness with resolution finer than the size of single IL ions. If layering is present in the liquid it is detected as alternating repulsive and attractive forces as D decreases (*e.g.* see Fig. 2b): Repulsions correspond to whole numbers of molecular layers, rendering the film 'stable' and therefore resisting squeeze out, and attractions in between are due to the surfaces being 'sucked together' as molecules are expelled. These alternating (oscillatory) repulsions and attractions are called structural forces,[42] and have been observed for non-polar molecular liquids which also form layered structures in thin films.

The first of these SFA experiments demonstrated layered structure in a protic IL, ethylammonium nitrate ([EA][NO_3]), confined between two (negatively charged) mica surfaces.[37] Since [EA][NO_3] is fully miscible with water in all proportions at room temperature, it was possible to show the layered structure emerging as the [EA][NO_3] concentration in water increases: at low concentrations of [EA][NO_3] the solution behaves as a simple electrolyte (with no ordered ion packing), then structure begins to be detected at 50% [EA][NO_3] and increases until 8-9 ordered layers are detected between the surfaces in pure [EA][NO_3]. The distance between the repulsive walls—or the period of oscillation—was similar to the dimension of the ion pair. From this we can conclude that each oscillation in force represents a layer of cations and a layer of anions being squeezed out together (or, equivalently, a single 'ion pair layer'; see later). It is worth noting the important distinction between the structural forces observed for molecular and ionic liquids: whereas for molecular liquids each oscillation in force corresponds to the squeeze-out of one molecular layer,[42] for ILs an oscillation corresponds to squeeze-out of an ion-pair layer as required to maintain electro-neutrality in the confined film.

More recently, experiments in the groups of Perkin,[38,39] Kurihara,[40] and Bureau[41] have all investigated the structuring of non-protic IL confined to films between charged surfaces (see Fig. 2b). ILs studied were [C_4C_1im][NTf_2],[39,40] [C_4C_1im][BF_4],[40,41] [C_4C_1im][PF_6],[41] [C_2C_1im][C_2SO_4],[38] and [C_6C_1im][NTf_2],[39] and the solid confining walls used were mica,[38–39,41] silica,[40] and a methyl-terminated monolayer[41] (see Table 1 for IL structures). For the mica and silica substrates (both negatively charged)

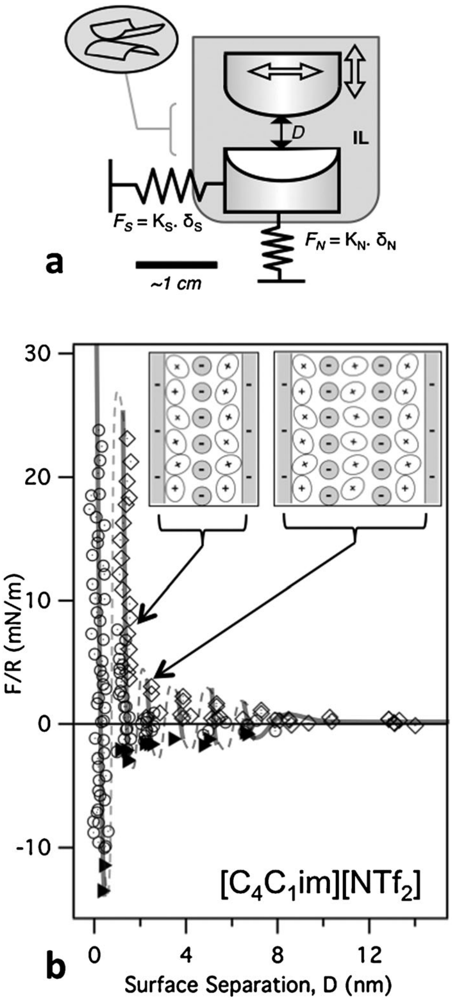

Fig. 2 ILs are studied in thin films between atomically smooth surfaces in a surface force balance or surface force apparatus (SFB/SFA). (a) Schematic setup of the SFB, showing the mica substrates in crossed-cylinder arrangement to study a thin film of liquid between them. One surface is moved relative to the other and the interaction force, as a function of separation distance, D, is measured through the bending of springs. (b) Measured force, F_N, between two mica surfaces (normalised by the mica curvature, R) *versus* film thickness, D, for [C$_4$C$_1$im][NTf$_2$] measured in the SFB. Open diamonds indicate points measured on approach of the surfaces (decreasing D) while open circles indicate data measured on retraction of the surfaces. Filled triangles indicate points measured from the jump-apart of the surfaces from an adhesive minimum. The lines are a guide to the eye to show the oscillatory nature of the forces, with solid lines through measured regions and dashed lines through the regions inaccessible to measurement due to the jump-in from the previous energy barrier. The inset cartoons show examples (for just two of the repulsive force 'walls') of the interpretation of the oscillatory forces: force walls–which correspond to energy minima–are due to stable films containing odd numbers of ion layers, alternating between cation and anion-rich layers with cations at each of the negatively charged surfaces. These simplified cartoons do not show how the excess of anions and cations decreases away from the surfaces. Adapted from Perkin *et al.*[39]

the results are qualitatively similar for all ILs studied, and when the same IL was studied in different laboratories the agreement in D-values is also quantitative (small differences in force are attributed to the difference in negative charge on mica *vs.* silica). The common features observed are as follows: (i) structural forces—oscillations between repulsive and attractive force—are apparent from $D \approx 5$–10 nm down to the smallest D reached, with increasing magnitude as D decreases; (ii) the period of oscillations is commensurate with the estimated ion-pair size; (iii) ultimate repulsion is measured at small D, which is not overcome despite applying large normal force. In the cases where sub-nanometre distances were accessed, this ultimate repulsion occurred at D-values smaller than the ion-pair size and commensurate with the cation size. One other group has studied ILs between mica surfaces,[43] although film thicknesses below $\sim$ 5 nm were not studied and structural forces were not clearly shown.

These features lead to a general interpretation of the layering of IL between charged (mica or silica) surfaces, as follows. IL is arranged in layers adjacent to charged surfaces, with $\sim$ 3–10 layers distinguishable before the liquid becomes bulk-like. The first layer adjacent to each negatively charged surface contains cations attracted electrostatically to screen or neutralise the surface charge. The subsequent layers are of a thickness similar to the ion-pair length and are likely to be made up mostly of ion-pair 'dipoles' aligned perpendicularly to the surface (with gradually decreasing 'purity of structure' away from the surface). That is to say, the layers contain two sub-layers (at least for the nearest-surface layers), with alternating anion sub-layer and cation sub-layer (Fig. 2b, inset). The origin of this alternating charge density away from the surface is the overscreening effect expected in dense ionic systems:[24,35,44] the surface negative charge pulls 'too many' cations into the first layer, the next layer over-compensating with anions, and so on (with gradually decreasing magnitude) for several layers. The higher magnitude of force at small D tells us of the stronger ordering of the layers closest to the interface. The observation that a large positive force is required to expel the liquid layers indicates a strong cohesive interaction between IL and surface and between IL layers (compared, for example, to uncharged molecular liquids which are squeezed out at significantly lower force[11]). This is likely due to a combination of dispersion interactions, significant for these polarisable ions, and electrostatics.

Of relevance to all IL physical chemistry, and in particular to high-resolution surface studies, is the question of impurities present in the liquid and their possible effect on experimental results. For example impurities such as oxides of aluminium or silicon can be incorporated into the IL during purification steps in its synthesis and have been shown to lead to unexpected surface effects in the past.[45,46] An important advantage of the SFA/SFB technique is the *absolute* measurement of D, which means that contamination at the surfaces, if present, is usually unambiguously detected: particulate impurities are immediately seen as they cause a long-range repulsion which obscures any oscillatory forces. Experiments revealing contamination are discarded, and high standards of IL purity are required in order to observe the IL surface layering discussed above. Another possible source of contamination is the mica substrate most commonly used for SFA/SFB experiments. These are prepared by cleavage along the crystal plane in clean (laminar flow) lab conditions, and it has been shown that

Table 1 Full names and structures for the ILs discussed in the text

Ionic liquid	Full name	Cation	Anion
$[C_1C_1im][Cl]$	1,3-dimethylimidazolium chloride	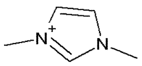	Cl^-
$[C_2C_1im][C_2SO_4]$	1-ethyl-3-methylimidazolium ethylsulfate	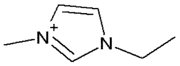	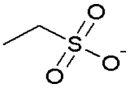
$[C_2C_1im][SCN]$	1-ethyl-3-methylimidazolium thiocyanate	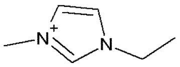	$S{=}C{=}N^-$
$[C_4C_1im][NTf_2]$	1-butyl-3-methylimidazolium bis(trifluoromethylsulfonyl)imide	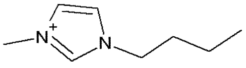	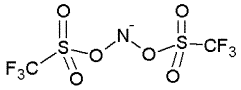
$[C_4C_1im][BF_4]$	1-butyl-3-methylimidazolium tetrafluoroborate	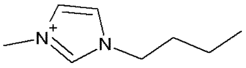	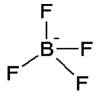
$[C_4C_1im][PF_6]$	1-butyl-3-methylimidazolium hexafluorophosphate	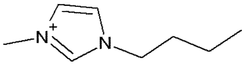	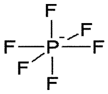
$[C_4C_1im][NTf_2]$	1-hexyl-3-methylimidazolium bis(trifluoromethylsulfonyl)imide	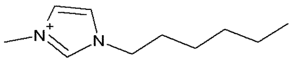	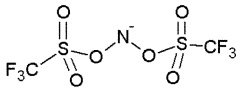
$[EA][NO_3]$	ethylammonium nitrate	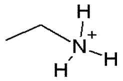	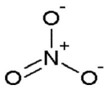

adsorption of H_2O and CO_2 from the air rapidly leads to a contaminant layer (of thickness ~ 0.5 nm), containing potassium carbonate.[47,48] This layer is removed in water, and from the *D*-values in IL experiments and from the solubility of K^+ and CO_3^- in the ILs it is inferred that this layer is also removed (dissolved) in the IL. Importantly, SFA/SFB experiments are performed with a 'reservoir' of bulk IL in contact with the thin film, so that K^+ ions from the surface, once dissociated, become negligible in concentration in the surface or film region.

2.3. Amphiphilic ionic liquids lead to self-assembly

An exception to the alternating cation/anion layer structure has been observed for an IL with a longer hydrocarbon chain on the cation, rendering the cation more amphiphilic.[39] In this case the driving force of amphiphile self-assembly competes (and wins) against the pure electrostatics, leading to a tail-to-tail cation bilayer structure (Fig. 3). This interfacial self-assembly, or formation of cation bilayer structures in confinement, has not yet been tested in simulations although aggregation of hydrocarbon tails into non-polar domains has been seen at a single interface.[30] It appears that although the alternating cation/anion structure is the dominant structure in thin films, observed for a range of 'simpler' ILs, it is not ubiquitous and can be disrupted by stronger ordering driving forces such as the collecting together of non-polar and polar moieties.

2.4. Simulations of ionic liquid in slit-pore geometry

Atomistic simulations have provided a complementary view of the structure of ILs confined to slit-pore geometries.[49–52] Between uncharged walls $[C_1C_1im][Cl]$ is found to form layers with a high density layer closest to the surface.[49] The first layer is cation-rich and the next layer is anion-rich, despite the absence of any charge on the surfaces. This suggests that the preference of imidazolium cations for the surface—as also observed in the experiments described above with negatively charged surfaces—may be partly driven by favourable packing of the ions in the vicinity of the surface rather than pure electrostatics. When charge is applied to the confining surfaces the ions translate in order to screen the charge. Distinct ion movement occurs at the anode resulting in layers of anions and cations, while at the cathode segregation occurs to a lesser extent.[50] These observations might be rationalised in light of the particular ions studied: the small Cl- anion can more easily fit into a first layer next to the surface without perturbing the cation layer.

Whilst the ions form distinct layer structures in the direction perpendicular to the confining surfaces, no increase in order compared to the bulk liquid was found in the plane of the layers for films of $[C_1C_1im][Cl]$ greater than 2.5 nm thickness.[49] On the other hand, when the same IL is confined to films thinner than 1.1 nm, corresponding to bilayer and monolayer films, it was found to crystallize with in-plane long range order observed in the radial distribution functions.[51,52]

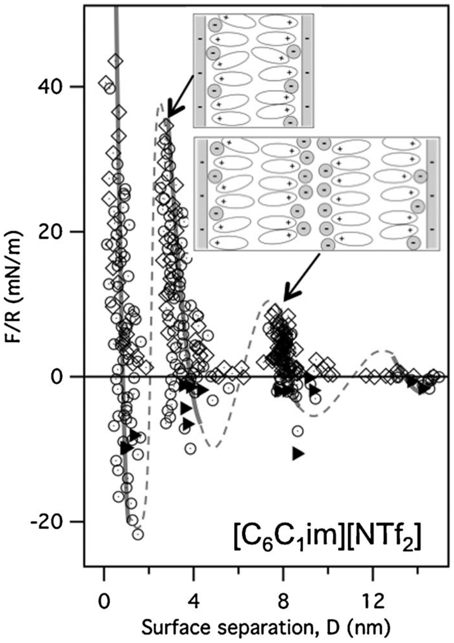

Fig. 3 Measured force, F_N, between two mica surfaces (normalised by the mica curvature, R) *versus* film thickness, D, for $[C_6C_1im][NTf_2]$. The symbols and lines are as defined in Fig. 2. The inset cartoons show examples (for two of the repulsive walls) of the interpretation of the oscillatory forces in this case: due to the amphiphilic nature of the IL the most stable films (*i.e.* force walls) occur where tail-to-tail bilayers stack between the two solid surfaces. Lamellae of non-polar and charged regions are formed. Adapted from Perkin *et al.*[39]

2.5. Future directions

Experiments with precisely controlled confinement geometry have been carried out, studying a small range of protic and non-protic ILs. A picture emerges of the typical structure of ILs confined between two charged solid walls of ions arranged in ion-pair dipole layers. Given their relevance to many applications, we would like to know what is the effect of surface charge, or of surface chemical groups, on the structure of the confined IL. For example the application of ILs as supporting electrolytes in supercapacitors requires knowledge of the EDL structure in the confined pores of the nanostructured electrode: the ordering of cations and anions, their orientations relative to the electrode surfaces, and how these are altered when the electrode voltage changes, must be optimised. It is clear from the above SFA experiments that the effect of ion and surface type can be dramatic;[39–41] and AFM experiments with a single Au substrate of varying potential show that the number of ion layers as well as their binding tenacity are dependent on surface applied voltage.[33] However experiments with both well defined confinement geometry and precisely known (and varying) surface charge have not to date been carried out and this represents an important direction for future work.

3. Dynamics of confined ionic liquids

The dynamic properties of molecular (non-ionic) liquids in nano-confinement have been extensively studied; in contrast only a few recent studies—motivated by the desire to understand motion of ions in the pores of nanoporous electrode materials and as friction modifiers—describe the dynamics of confined ionic liquids. Already from this early work it is apparent that ionic liquids display at least as rich a landscape as molecular liquids, with dramatic differences in dynamic behaviour arising from changes in the surface charge, surface chemistry, and film thickness.

3.1. Dynamics in model thin films

SFA or SFB experiments have been able to detect fluidity and dynamics of confined ILs at the same time as providing absolute characterisation of the confinement geometry.[38,40,41] In addition to measuring the thickness of the IL film, D, with a resolution of single ion interfacial layers, dynamic SFA experiments provide extra information such as friction coefficient or viscosity as a function of the number of ion layers between the two confining surfaces. By gradually reducing D from micrometres down to a few molecular layers, the point at which the dynamic properties change can be detected. These dynamic properties of the confined liquid can be measured one of two ways: Firstly, a lateral shearing motion can be applied to one confining surface and the coupling across the liquid to the other surface is then detected *via* a lateral spring ('shear method'). Secondly, the surfaces can be moved towards each other and the viscous drag experienced due to the flow of liquid out of the film is detected as a hydrodynamic force ('hydrodynamic method'). Experiments in three laboratories[38,40,41] have studied the effect of confinement on viscosity of a small number of ionic liquids, using the shear and hydrodynamic methods, and the results are summarised as follows. In the Kurihara group, SFA experiments using silca surfaces and two imidazolium-type ionic liquids, $[C_4C_1im][NTf_2]$ and $[C_4C_1im][BF_4]$, revealed changes to the dynamic properties of the liquid when D was decreased below 7-8 nm.[40] This distance corresponded with the onset of structural forces (see section 2), leading to the conclusion that the changing dynamics are caused by the confinement-induced structuring of the liquid. It was shown using the shear method that for films thinner than 7-8 nm the viscosity increased exponentially with decreasing D, ultimately reaching values $\sim$ 3 orders of magnitude greater than the bulk viscosity at $\sim$2 nm. In the Bureau group, SFA experiments using mica surfaces and two imidazolium-type ionic liquids, $[C_4C_1im][PF_6]$ and $[C_4C_1im][BF_4]$, revealed changes to the dynamic properties of the liquid when D was decreased below 20 nm.[41] Using the hydrodynamic method, the viscosity was seen to reduce by one order of magnitude as D decreased from $\sim$ 20 nm to $\sim$ 5-6 nm. Below 5 nm, the shear method revealed further increase of viscosity over several orders of magnitude dependent on the shear rate. For films below 2.5 nm ($[C_4C_1im][PF_6]$) or 3.5 nm ($[C_4C_1im][PF_6]$) a yield shear stress was observed, indicating solid-like behaviour of the film. In the Perkin group, SFB experiments using mica surfaces and one IL, $[C_2C_1im][C_2SO_4]$, used the shear method to demonstrate an increase of viscosity over two orders of magnitude as the IL was confined down to D $\sim$ 1 nm; interpreted as three ion layers between the mica surfaces.[38]

Thus these high-resolution dynamic experiments, using different methods of measurement and probing several ILs, provide general agreement on the following dynamic features of ILs confined to thin films: (i) the IL remains liquid-like, retaining bulk viscosity, in films thicker than ~ 10–20 nm; (ii) viscosity of the confined IL increases by 1–3 orders of magnitude as the liquid is confined from ~ 5–20 nm down to ~ 1–3 nm (precise thicknesses depending on the IL and the surface); (iii) some solid-like characteristics (*e.g.* finite shear stress) are observed for the thinnest films (~ few nm, corresponding to only a few ion layers). Despite the increase of viscosity and the emergence of shear stress for thin IL films, ions in the film remain significantly mobile relative to ILs undergoing bulk glass transition or solidification: a viscosity increase of 1–3 orders is small compared to the ~ 10 orders expected at bulk solidification.

What is the cause of the increase in viscosity observed in the SFA experiments? Two observations suggest that the ion layering structure causes the enhanced viscosity. Firstly, the onset distance of the changing viscosity matches the distance at which structural forces are observed.[38,40,41] Secondly, when the surfaces bear no charge and do not induce any structuring there is concomitantly no increase in viscosity.[41] We point out that it is likely the non-isotropic structure of confined IL causes anisotropy of the dynamic properties: ion diffusion and structure relaxation within each layer involves different molecular interactions and energy barriers compared to diffusion between layers. This is analogous to the anisotropic viscosity of liquid crystalline systems, leading to three so-called Miesowicz viscosity coefficients.[53,54] Thus it is possible that the two methods used to probe dynamics in SFA experiments above—the shear method and hydrodynamic method—will lead to differences in the observed onset distance of dynamic changes and even the viscosities probed: since the IL is aligned in layers parallel to the confining surfaces, shearing the film laterally could occur without disrupting the layer structure; whereas pushing the surfaces together to squeeze out the liquid must cause the layer structure to be disrupted. This may explain why an increase in viscosity above the bulk value is probed from ~ 20 nm using the hydrodynamic method, and from smaller distances (5–10 nm) using shear methods.

Further insight into the molecular origin of confinement-induced dynamic changes comes from molecular dynamic simulations. A simulation of [C_4C_1im][PF_6] confined to a graphite slit-pore of width 5.4 nm showed that IL dynamics are heterogeneous across the confined film, depending strongly on the distance of the ions from the walls:[55] The first layer of ions adjacent to each interface are dramatically slowed, the next layer are slowed to an intermediate extent, and the remaining IL in the middle of the pore is more similar to bulk IL. Additionally, the ions were seen to diffuse primarily within their layers, *i.e.* parallel to the walls, whereas diffusion of ions from one layer to the next (motion perpendicular to the walls) was slower.[49,55] This conclusion is supported by a simulation of [C_4C_1im][NTf_2] confined to a cylindrical pore of diameter 4.8 nm which revealed 'stiffening' of the few layers at the interface whilst ions in the centre of the pore have bulk-like self-diffusion and conductive properties.[56] Another simulation confining the IL to even thinner films, where only a monolayer or bilayer remains between solid walls, showed solidification of the film although this was for the higher melting point salt [C_1C_1im][Cl].[51,52] In contrast, a simulation with uniform (un-corrugated) solvophobic walls showed faster motion near the walls than in the bulk, revealing the importance of surface-IL interactions and chemistry for ion dynamics.[49]

3.2. Dynamics in mesoporous networks

The SFA and simulation studies discussed above involved model systems with finely controlled pore or film thickness and surface chemistry. A number of other experimental studies have used more heterogeneous systems such as mesoporous silica, allowing the dynamics of IL confined within these network of pores to be probed using NMR, DSC and conductivity. For example ion dynamics in pores was probed by recording the conductance through a single conical nanopore in a membrane: for a 20 ± 2 nm pore radius, conductivity can be either enhanced (for [C_4C_1im][NTf_2]) or conversely halted (for [C_2C_1im][SCN]) relative to bulk transport.[57] The dynamics of IL in a mesoporous silica network with pore sizes between 5 and 50 nm were probed with IR and ^{1}H NMR; resulting spectra showed no (or little) slowing of the ion dynamics due to confinement and it was concluded that ILs in the pores behaved like the bulk liquid.[58,59] IL confined to pores in a more hydrophobic (methyl terminated) ionogel network also maintained bulk-like ion conductivity.[60] Confinement to these mesoporous networks can alter IL phase behaviour, for example leading to melting point depression, in particular for the narrowest pore sizes (~ 5 nm).[58–62] Confinement of [C_4C_1im][PF_6] into multi-walled carbon nanotubes resulted in entirely different behaviour: the IL solidifies at room temperature and the melting point increases to above 490 K.[63] In light of the SFA experiments—which showed slower ion dynamics only in the few layers closest to the walls—we might expect ILs to maintain bulk liquid-like properties in porous networks when the pore size is on the order of 10 ion diameters or greater, and thus where a large fraction of the liquid is far from the walls. When the pore size is smaller some retardation of ion dynamics and changes to phase properties may be observed, in particular when the pore size is reduced to just a few ion diameters. It is also possible that polydispersity in pore size in the mesoporous networks contributes to the observed ion dynamics—only a few much larger than average pores are required to host a large fraction of the liquid—and may lead to apparent discrepancies with model experiments.

3.3. Lubrication by ionic liquids

The potentially major application of ILs as lubricants, either in pure form or as additives, has been demonstrated using conventional macroscopic ball-on-plate or pin-on-disk tribometers.[5,7,64–68] The performance of a liquid lubricant depends on a number of factors including its viscosity and phase behaviour in thin films, strength of molecular interaction between the liquid and the shearing solid surfaces, thermal stability, volatility, and others. Particularly pertinent are lubricants for micro- and nano-electromechanical devices (MEMS) where the lubricant should be molecularly thick, bound to the device surface and highly durable and reproducible in its behaviour.[69,70] ILs are a promising source of these so-called 'boundary lubricants' due to their non-volatility, excellent thermal stability up to high temperatures and potential for electrostatic and van der Waals interactions with the surfaces. However in order to exploit these characteristics it is desirable to understand the effect of IL chemical structure on shear stress and friction coefficient of a confined thin IL film when sheared between two solid surfaces.

The chemistry of the IL and surface functional groups has been shown to alter the friction of sliding surfaces across IL films. For example, longer alkyl chains were found to be preferred for lower friction; and pyridinium-based ILs resulted in lower friction than imidazolium-based ILs.[71] The stronger the interaction between IL functional groups and the surface the lower the friction, with carboxylic acid groups giving the lowest value.[72,73] Vinyl groups can help control the stability of the IL under high pressure and temperature.[65,74] The effect of cation valency on friction was studied by Palacio *et al.*,[75] who showed that ILs composed of di-valent cation and mono-valent anion (2 : 1) could exhibit either lower or higher friction coefficient compared to a 1 : 1 IL: the 2 : 1 IL with a hydrophobic linker between the two positively charged groups showed significantly improved lubrication capacity, whereas the 2 : 1 IL with a hydrophilic linker was not so effective. Altering the surface chemistry by anchoring the cation of the IL to the surface can improve the tribological performance of the surface, moreover the counter (an)ion can be varied to control the friction coefficient on the modified surface.[76]

The structure of an IL boundary lubricant film has been shown in two cases ($[C_2C_1im][C_2SO_4]$ and $[EA][NO_3]$) to consist of 1–3 ion layers, depending on the applied load.[38,77] At lower applied load, where 2-3 ion layers were present, the friction, F_S, was very low and independent of sliding speed (v_S). Increasing the load led to a decrease in the film thickness to one ion layer between the surfaces; F_S and the friction coefficient, μ, then increased in magnitude and became velocity dependent.[77] At the highest loads μ again became independent of v_S.

3.4. Three regimes of IL boundary lubrication

Bringing together the evidence from the small number of studies of friction and dynamics to date, some tentative suggestions can be made about general mechanisms of lubrication by ILs. In the hydrodynamic regime, ILs perform as lubricants on the basis of their viscosity and reluctance to solidify in films greater than a few nm thickness. Once confined to thinner films, of a few ion layers, ILs exhibit some notable properties as boundary lubricants as a result of their charge, polarisability, amphiphilicity, and layering tendency which differentiate them from other lubricants. In this context, we suggest that the film be considered as a boundary lubricant if it is entirely composed of ordered ion layers and therefore no 'bulk' IL is present. It is useful to consider the resulting boundary lubrication within three regimes which can be summarised as follows:

(i) At low loads and slow shear rate, the boundary film has in-layer relaxation times faster than the shear rate resulting in low F_S and μ, with μ independent of v_S.

(ii) At higher loads, where the boundary film relaxation is slowed due to greater confinement (fewer ion layers) or molecular interdigitation, there is an intermediate regime: F_S is higher and μ is dependent on v_S.

(iii) At the highest loads and therefore thinnest boundary films (typically one ion layer), no ion diffusion or molecular relaxation can occur on the timescale of shearing and the surfaces move laterally by way of slip along a shear plane. μ is again independent of v_S. F_S can be lower or higher than in (ii).

Switching from one regime to the next occurs at certain critical values of normal load, F_N (or velocity, v_S). As load is increased, switching will be associated with structural changes in the film such as squeezing out of an ion-pair layer or reorganisation within a layer. Regime (i) will typically apply to films consisting of more than one ion layer because the ions in the first layer are bound to the surfaces and have slower relaxation; dissipation occurs by ion motion within the mid-layer(s) of ions. Examples are the three ion layers ('$n = 3$') film of $[C_2C_1im][C_2SO_4]$ between mica sheets[38] and $\geq$ 2 ion layers of $[EA][NO_3]$ (or one [EA] cation layer, for the slowest v_S applied).[77] Regime (ii) occurs when the molecular reorganisation timescale is similar to the shear rate of the experiment and so will be sensitive to small changes in temperature, velocity and load. Regime (iii) consists of a solid-like film of ions between the shearing surfaces, and since slip must occur at the plane between the ions and surface the friction in this regime is most sensitive to the particular IL-surface interaction and could be either lower or higher than in regime (ii).

This friction phase analysis is similar to that applied in the past to boundary surfactant films.[42,78] However ILs are worth considering independently from other boundary lubricants for several reasons. Firstly, their charge-induced layering structure of alternating cations and anions means that one or more ion layers can be considered to be part of the boundary layer. The relaxation processes occurring to dissipate friction can involve ion motion within one ion layer without ion diffusion between layers. And electrostatic interactions between charged surfaces and (counter-)ions in the IL film prevent squeeze-out of the boundary ion layers, resulting in the high load-bearing capacity of ILs compared to non-polar liquids.[38] Finally, slip can occur at the IL-surface plane (as well as at any of the other IL-IL layer interfaces if more than one ion layer is present). Whilst this rich phase behaviour of ILs as boundary lubricants is hinted at by the few studies undertaken to date, much work remains to be done if we are to be able to relate IL chemistry to boundary friction and eventually to predict and tune IL boundary lubricants for specific applications.

4. Colloidal forces and particle stabilisation in ionic liquids

4.1. IL as a dispersion medium

Using ionic liquid as the solvent for dispersion of colloidal particles and for the generation and stabilisation of metal nanoparticles is proving a useful route to a vast array of new functional materials.[79–81] Dispersions of transition metal nanoparticles, for example, are effective as nano-catalysts and bridge the classical division of homogeneous and heterogeneous catalysts.[82,83] Colloidal silica dispersed in IL can be transformed into colloidal gels or colloidal glasses, with unique combinations of conductive, optical and rheological properties.[79,84,85] An example is the gelation of silica suspended in IL to create solid yet conducting electrolytes for solar cell applications.[86] Quantum dot nanoparticles dispersed in ILs display a remarkable enhancement of photoluminescent properties, and have potential applications in optoelectronic devices.[87] Carbon nanotubes can also be dispersed in ILs—of particular note since nanotubes tend to aggregate in most molecular solvents—which has led to new 'bucky-gel' materials[9] and novel electronics.[8]

Particles dispersed in IL without added stabilisers such as surfactants or polymers might, at first thought, be expected to be unstable with respect to aggregation: after all, IL is a maximally concentrated salt, and the classical DLVO theory of colloid stability predicts that particles immersed in a medium of high salt concentration will aggregate due to the attractive van der Waals force between them and the screening of repulsive electrostatic interactions.[88] However, whilst the DLVO theory (after Derjaguin, Landau, Verwey and Overbeek) is remarkably effective at explaining and predicting interaction forces in many cases, this mean-field theory does not take into account excluded volume or steric effects which can dominate at high (or even moderate) salt concentrations.[89–91] In IL media the Debye screening length calculated from the ion concentration and dielectric constant would be ~ 1-2 Å; however it is impossible for screening of a surface charge by IL to occur over this length scale which is significantly smaller than a single IL ion diameter. In order to explain the many examples of particle stability in IL media mentioned above it is clear that we need to consider additional interactions not accounted for in mean-field theories.

4.2. The forces acting between particles in IL

The interaction energy (and force) between particles across an IL medium, as a function of separation distance, is a convolution of several effects: electrostatic and van der Waals forces, as well as steric repulsions, solvation forces, and osmotic interactions due to polymers (if present) at the particle surface. The relative range and form of each of these interactions is indicated in Fig. 4b. Direct electrostatic interactions are highly screened by the IL, as discussed above, and so act only when the particles are at very close separation. Steric repulsions occur when molecules adsorbed to a particle surface acts to prevent contact with another particle. Amphiphiles added to stabilise a dispersion can act in this way, as can amphiphilic ions of the IL itself; the range of this repulsion is the length of the adsorbed molecule. Solvation forces, on the other hand, can act from particle separations of order ~ 10 nm[37–41] (see section 2). Solvation forces between macroscopic surfaces are oscillatory—alternating between repulsion and attraction as separation distance is decreased—and so can contribute to either stabilisation of a dispersion or flocculation depending on the relative magnitudes of the thermal energy of the system and the oscillatory force. These oscillatory solvation forces, as measured between macroscopic surfaces and arising from squeeze out of ion layers as the surfaces approach, are likely to act between all colloidal particles and nanoparticles as long as the particle is significantly larger than the size of the IL ion size. For smaller nanoparticles the curvature of the particle surface may lead to different preferential ion packing in the vicinity and thus different solvation forces. In a simulation study of Ru nanoparticles of 2 nm diameter in $[C_4C_1im][NTf_2]$ the cations and anions were both present in the first layer adjacent to the metal surface; it was proposed that stabilisation of these nanoparticles is by way of the IL acting as a structural template.[92,93] Nanoparticles of ~ < 3 nm could fit within polar or non-polar domains, or pockets, in the IL structure—dependent on the particle surface polarity—with ion-ion interactions in the liquid not much disrupted by the presence of the nanoparticle. If polymers are added to the IL solvent then osmotic attractive or repulsive interactions will also act between the particles: for example dense surface-adsorbed or grafted polymers for which the IL is a good solvent will lead to long range repulsions (and stabilisation of the dispersion), while non-adsorbing polymers can cause particle aggregation due to depletion forces.[79]

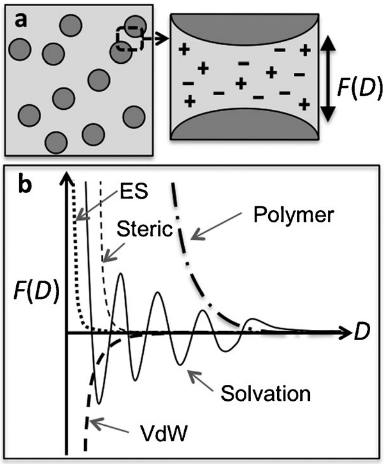

Fig. 4 (a) The stabilisation of nanoparticles and colloidal particles in IL depends upon the change in interaction energy with distance, *i.e.* force, between the particles across the intervening film of anions and cations. (b) The forces acting include van der Waals forces ('vdW', bold dashes), screened electrostatics ('ES', dotted line), steric interactions ('steric', fine dashes), solvation forces ('solvation', solid line), and interactions due to adsorbed or grafted polymers ('polymer', dot-dash line); relative forms and ranges of these are shown here and discussed in the text.

For any particular combination of nanoparticle material, surface charge, particle size, and IL structure, a different combination of these forces will be acting, leading to a unique 'force law' between the particles. For example charged solvophilic surfaces tend to induce solvation forces with the oscillations showing more repulsive than attractive character.[37,39,40] When the surface charge is higher, the oscillatory solvation force can be amplified.[33] On the other hand uncharged solvophobic surfaces lead to more attractive solvation forces across IL.[31,41] A challenge for future work lies in quantifying these effects and distinguishing between the roles of charge, chemical groups and particle size, and subsequently predicting and controlling the stability of particle dispersions in IL.

5. Concluding remarks

Motivated by the many applications of ILs in confined geometries—as electrolytes, lubricants, and dispersants—the

SFA has been adapted to study their structure and properties with molecular resolution. By comparing several recent experimental studies, as well as molecular dynamics simulations, some general features of ion arrangements and dynamics in confined geometries have been identified.

The interaction force between two identical atomically smooth and negatively charged surfaces across IL films was found to be an oscillatory function of the film thickness. Energy minima, corresponding to favourable ion-packing arrangements in the film, revealed how—for typical ILs between charged surfaces—the liquid is arranged in ion-pair layers parallel to the solid surfaces. Non-polar surfaces were found to disrupt the ion packing so that layering is not observed, and ILs with amphiphilic character appear to stack in bilayers rather than ion-pair layers in the film. Despite strong ordering in the direction perpendicular to the surfaces, the IL does not crystallize and long range order is not observed within each plane or ion layer.

Dynamic SFA experiments and MD simulations have demonstrated an increase in viscosity of 1–3 orders of magnitude relative to the bulk for ILs confined to films of 1–3 nm, caused by the enhanced structure in the film in the direction perpendicular to the surfaces and interactions between the ion layers adjacent to the walls. Despite some increase in viscosity, these thinnest IL films act as highly efficient boundary lubricants. Three regimes have been outlined, each relating to a different mechanism of boundary lubrication. Early work has shown that the charge-induced layering of ILs leads to unique and interesting dynamics in thin films; it remains a challenge to relate IL chemical structure to quantitative dynamics.

Dispersions of nanoparticles, carbon nanotubes, and other colloidal materials in IL have been shown to follow different rules of colloidal stability to the DLVO-type behaviour of dilute aqueous solutions. SFA experiments revealed the range of interactions of two solid surfaces across IL to be up to $\sim$ 10 nm; significantly greater than predicted with mean-field electrostatics. Solvation forces were shown to be primarily responsible for these long-range interactions, although it is not yet clear how the interplay between surface charge on the particle, IL shape and size, amphiphilicity, and other parameters determine their range and magnitude. Experiments with a wider range of ILs and surface materials will help to elucidate these, and ultimately to rationalise quantitatively the stability of colloids in ILs.

Acknowledgements

The Leverhulme Trust (grants F/07 134/DK and F/07 134/DN), Weizmann UK, and the US Office of Naval Research (N000141010096) are gratefully acknowledged for financial support. I am grateful to an anonymous referee for raising an interesting point relating to ion layering.

References

1 M. Armand, *et al.*, Ionic-liquid materials for the electrochemical challenges of the future, *Nat. Mater.*, 2009, **8**(8), 621–9.

2 P. Simon, *et al.*, Materials for electrochemical capacitors, *Nat. Mater.*, 2008, **7**(11), 845–54.

3 Y. Bai, *et al.*, High-performance dye-sensitised solar cells based on solvent-free electrolytes produced from eutectic melts, *Nat. Mater.*, 2008, **7**, 626–30.

4 Y. Zhu, et al., *Carbon-Based Supercapacitors Produced by Activation of Graphene Science*, 2011, **332**(6037), 1537–41.

5 C. Ye, *et al.*, Room temperature ionic liquids: a novel versatile lubricant, *Chem. Commun.*, 2001, 2244–5.

6 W. Liu, *et al.*, Tribological performance of room-temperature ionic liquids as lubricant, *Tribol. Lett.*, 2002, **13**(2), 81–5.

7 F. Zhou, *et al.*, Ionic liquid lubricants: designed chemistry for engineering applications, *Chem. Soc. Rev.*, 2009, **38**(9), 2590–9.

8 T. Sekitani, *et al.*, A rubberlike stretchable active matrix using elastic conductors, *Science*, 2008, **321**(5895), 1468–72.

9 T. Fukushima, *et al.*, Molecular Ordering of Organic Molten Salts Triggered by Single-Walled Carbon Nanotubes, *Science*, 2003, **300**(5628), 2072–4.

10 J. Klein, *et al.*, Confinement-induced phase transitions in simple liquids, *Science*, 1995, **269**, 816–9.

11 J. Klein, *et al.*, Simple liquids confined to molecularly thin layers. I. Confinement-induced liquid-to-solid phase transitions, *J. Chem. Phys.*, 1998, **108**(16), 6996–7008.

12 U. Raviv, *et al.*, Fluidity of water confined to subnanometre films, *Nature*, 2001, **413**, 51–4.

13 U. Raviv, *et al.*, Fluidity of bound hydration layers, *Science*, 2002, **297**, 1540–3.

14 U. Raviv, *et al.*, Fluidity of water confined down to sub-nanometer films, *Langmuir*, 2004, **20**(13), 5322–32.

15 J. N. A. Canongia Lopes, *et al.*, Nanostructural Organization in Ionic Liquids, *J. Phys. Chem. B*, 2006, **110**(7), 3330–5.

16 S. Urahata, Structure of ionic liquids of 1-alkyl-3-methylimidazolium cations: A systematic computer simulation study, *J. Chem. Phys.*, 2004, **120**(4), 1855.

17 Y. Wang, *et al.*, Unique Spatial Heterogeneity in Ionic Liquids, *J. Am. Chem. Soc.*, 2005, **127**(35), 12192–3.

18 A. Triolo, *et al.*, Nanoscale Segregation in Room Temperature Ionic Liquids, *J. Phys. Chem. B*, 2007, **111**(18), 4641–4.

19 B. L. Bhargava, *et al.*, Nanoscale orgainsation in room temperature ionic liquids: a course grained molecular dynamics simulation study, *Soft Matter*, 2007, **3**, 1395–400.

20 S. G. Raju, *et al.*, Emergence of nanoscale order in room temperature ionic liquids: simulation of symmetric 1,3-didecylimidazolium hexafluorophosphate, *J. Mater. Chem.*, 2009, **19**(25), 4343–7.

21 Nanostructure in ionic liquids (special issue), *Phys. Chem. Chem. Phys.*, 2011, **13**(30), pp. 13453–840.

22 M. Mezger, *et al.*, Molecular layering of fluorinated ionic liquids at charged sapphire (0001) surface, *Science*, 2008, **322**, 424–8.

23 M. Mezger, *et al.*, Layering of [BMIM] + based ionic liquids at a charged sapphire interface, *J. Chem. Phys.*, 2009, **131**(9), 094701–9.

24 M. V. Fedorov, *et al.*, Ionic liquid near a charged wall: structure and capacitance of electrical double layer, *J. Phys. Chem. B*, 2008, **112**(38), 11868–72.

25 M. V. Fedorov, *et al.*, Double layer in ionic liquids: The nature of the camel shape of capacitance, *Electrochem. Commun.*, 2010, **12**(2), 296–9.

26 O. J. Lanning, *et al.*, Screening at a Charged Surface by a Molten Salt, *J. Phys. Chem. B*, 2004, **108**(30), 11069–72.

27 M. Sha, *et al.*, Ordering layers of [bmim][PF6] ionic liquid on graphite surfaces: Molecular dynamics simulation, *J. Chem. Phys.*, 2008, **128**(13), 134504–7.

28 S. A. Kislenko, *et al.*, Molecular dynamics simulation of the electrochemical interface between a graphite surface and the ionic liquid [BMIM][PF6], *Phys. Chem. Chem. Phys.*, 2009, **11**(27), 5584–90.

29 G. Feng, *et al.*, Microstructure and capacitance of the electrical double layers at the interface of ionic liquids and planar electrodes, *J. Phys. Chem. C*, 2009, **113**(11), 4549–59.

30 M. Sha, *et al.*, Double-Layer Formation of [Bmim][PF6] Ionic Liquid Triggered by Surface Negative Charge, *Langmuir*, 2010, **26**(15), 12667–72.

31 R. Atkin, *et al.*, Structure in confined room-temperature ionic liquids, *J. Phys. Chem. C*, 2007, **111**, 5162–8.

32 D. Wakeham, *et al.*, Influence of Temperature and Molecular Structure on Ionic Liquid Solvation Layers, *J. Phys. Chem. B*, 2009, **113**(17), 5961–6.

33 R. Hayes, *et al.*, Double Layer Structure of Ionic Liquids at the Au(111) Electrode Interface: An Atomic Force Microscopy Investigation, *J. Phys. Chem. C*, 2011, **115**(14), 6855–63.

34 R. Hayes, *et al.*, Pronounced Structure in Confined Aprotic Room-Temperature Ionic Liquids, *J. Phys. Chem. B*, 2009, **113**(20), 7049–52.

35 M. Z. Bazant, *et al.*, Double Layer in Ionic Liquids: Overscreening versus Crowding, *Phys. Rev. Lett.*, 2011, **106**(4), 046102.

36 A. A. Kornyshev, Double-Layer in Ionic Liquids: Paradigm Change?, *J. Phys. Chem. B*, 2007, **111**(20), 5545–57.

37 R. G. Horn, *et al.*, Double-layer and solvation forces measured in a molten salt and its mixtures with water, *J. Phys. Chem.*, 1988, **92**, 3531–7.

38 S. Perkin, *et al.*, Layering and shear properties of an ionic liquid, 1-ethyl-3-methylimidazolium ethylsulfate, confined to nano-films between mica surfaces, *Phys. Chem. Chem. Phys.*, 2010, **12**(6), 1243–7.

39 S. Perkin, *et al.*, Self-assembly in the electrical double layer of ionic liquids, *Chem. Commun.*, 2011, **47**(23), 6572–4.

40 K. Ueno, *et al.*, Resonance shear measurement of nanoconfined ionic liquids, *Phys. Chem. Chem. Phys.*, 2010, **12**(16), 4066–71.

41 I. Bou-Malham, *et al.*, Nanoconfined ionic liquids: effect of surface charges on flow and molecular layering, *Soft Matter*, 2010, **6**(17), 4062–5.

42 J. Israelachvili, *Intermolecular and Surface Forces*, Academic Press, London, 3rd edn, 2011.

43 Y. Min, *et al.*, Measurement of Forces across Room Temperature Ionic Liquids between Mica Surfaces, *J. Phys. Chem. C*, 2009, **113**(37), 16445–9.

44 V. Demery, *et al.*, Overscreening in 1D lattice Coulomb gas model of ionic liquids, arXiv:1107.1050v1, 2011.

45 F. Endres, *et al.*, Probing Lithium and Alumina Impurities in Air- and Water Stable Ionic Liquids by Cyclic Voltammetry and In Situ Scanning Tunneling Microscopy, *Z. Phys. Chem.*, 2006, **220**(10), 1377–94.

46 A. Foelske-Schmitz, *et al.*, XPS analysis of activated carbon supported ionic liquids: Enhanced purity and reduced charging, *Surf. Sci.*, 2011, **605**(23–24), 1979–85.

47 S. Perkin, *et al.*, Forces between mica surfaces, prepared in different ways, across aqueous and nonaqueous liquids confined to molecularly thin films, *Langmuir*, 2006, **22**(14), 6142–52.

48 H. K. Christenson, *et al.*, Growth of ionic crystallites on exposed surfaces, *J. Colloid Interface Sci.*, 1987, **117**(2), 576–7.

49 C. Pinilla, *et al.*, Structure and Dynamics of a Confined Ionic Liquid. Topics of Relevance to Dye-Sensitized Solar Cells, *J. Phys. Chem. B*, 2005, **109**(38), 17922–7.

50 C. Pinilla, *et al.*, Polarization Relaxation in an Ionic Liquid Confined between Electrified Walls, *J. Phys. Chem. B*, 2007, **111**(18), 4877–84.

51 M. Sha, *et al.*, Drastic Phase Transition in Ionic Liquid [Dmim][Cl] Confined Between Graphite Walls: New Phase Formation, *J. Phys. Chem. C*, 2009, **113**(11), 4618–22.

52 M. Sha, *et al.*, Liquid-to-Solid Phase Transition of a 1,3-Dimethylimidazolium Chloride Ionic Liquid Monolayer Confined between Graphite Walls, *J. Phys. Chem. C*, 2008, **112**(47), 18584–7.

53 J. L. Sanders, *et al.*, Laser tweezers for determining anisotropic viscosity coefficients of nematic liquid crystals, *Optical Trapping and Optical Micromanipulation VII*, 2010, **7762**, 776221–9.

54 M. Miesowicz, The three coefficients of viscosity of anisotropic liquids, *Nature*, 1946, **158**, 27.

55 R. Singh, *et al.*, Heterogeneity in the Dynamics of the Ionic Liquid [BMIM +][PF6-] Confined in a Slit Nanopore, *J. Phys. Chem. C*, 2011, **115**(33), 16544–54.

56 B. Coasne, *et al.*, Loading-Controlled Stiffening in Nanoconfined Ionic Liquids, *J. Phys. Chem. Lett.*, 2011, **2**(10), 1150–4.

57 C. Tasserit, *et al.*, Pink Noise of Ionic Conductance through Single Artificial Nanopores Revisited, *Phys. Rev. Lett.*, 2010, **105**(26), 260602.

58 J. Le Bideau, *et al.*, Effect of confinement on ionic liquids dynamics in monolithic silica ionogels: 1H NMR study, *Phys. Chem. Chem. Phys.*, 2007, **9**(40), 5419–22.

59 R. Göbel, *et al.*, Surprisingly high, bulk liquid-like mobility of silica-confined ionic liquids, *Phys. Chem. Chem. Phys.*, 2009, **11**(19), 3653–62.

60 M.-A. Neouze, *et al.*, Ionogels, New Materials Arising from the Confinement of Ionic Liquids within Silica-Derived Networks, *Chem. Mater.*, 2006, **18**(17), 3931–6.

61 M. Kanakubo, *et al.*, Melting point depression of ionic liquids confined in nanospaces, *Chem. Commun.*, 2006, (17), 1828–30.

62 M. Waechtler, *et al.*, 2H and 19F solid-state NMR studies of the ionic liquid [C2Py][BTA]-d10 confined in mesoporous silica materials, *Phys. Chem. Chem. Phys.*, 2010, **12**(37), 11371–9.

63 S. Chen, *et al.*, Transition of Ionic Liquid [bmim][PF6] from Liquid to High-Melting-Point Crystal When Confined in Multiwalled Carbon Nanotubes, *J. Am. Chem. Soc.*, 2007, **129**(9), 2416–7.

64 M. Palacio, *et al.*, A Review of Ionic Liquids for Green Molecular Lubrication in Nanotechnology, *Tribol. Lett.*, 2010, **40**(2), 247–68.

65 B. Yu, *et al.*, Tribological properties of ultra-thin ionic liquid films on single-crystal silicon wafers with functionalized surfaces, *Tribol. Int.*, 2006, **39**(9), 879–87.

66 L. Zhang, *et al.*, Tribological Characteristics of Alkylimidazolium Diethyl Phosphates Ionic Liquids as Lubricants for Steel,ÄìSteel Contact, *Tribol. Lett.*, 2009, **34**(2), 95–101.

67 B. S. Phillips, *et al.*, Ionic Liquid Lubrication Effects on Ceramics in a Water Environment, *Tribol. Lett.*, 2004, **17**(3), 533–41.

68 J. Sanes, *et al.*, Ionic liquids as lubricants of polystyrene and polyamide 6-steel contacts. Preparation and properties of new polymer-ionic liquid dispersions, *Tribol. Lett.*, 2006, **21**(2), 121–33.

69 B. Bhushan, *Springer handbook of nanotechnology*, Springer Verlag, Heidelberg, 2007.

70 B. N. J. Persson, *Sliding Friction*, Springer-Verlag, 1998.

71 J. J. Nainaparampil, *et al.*, Ionic-Liquid Lubrication of Sliding MEMS Contacts: Comparison of AFM Liquid Cell and Device-Level Tests, *J. Microelectromech. Syst.*, 2007, **16**(4), 836–43.

72 N. Nooruddin, *et al.*, Semi-Empirical Molecular Modeling of Ionic Liquid Tribology: Ionic Liquid–Hydroxylated Silicon Surface Interactions, *Tribol. Lett.*, 2009, **36**(2), 147–56.

73 W. Robert Carper, *et al.*, Semi-Empirical Molecular Modeling of Ionic Liquid Tribology: Ionic Liquid,ÄìAluminum Oxide Surface Interactions, *Tribol. Lett.*, 2011, **43**(2), 163–8.

74 D. Li, *et al.*, Excellent lubrication performance and superior corrosion resistance of vinyl functionalized ionic liquid lubricants at elevated temperature, *Tribol. Int.*, 2011, **44**(10), 1111–7.

75 M. Palacio, *et al.*, Molecularly thick dicationic ionic liquid films for nanolubrication, *J. Vac. Sci. Technol., A*, 2009, **27**(4), 986–95.

76 J. Liu, *et al.*, Tribological Properties of Self-Assembled Monolayers of Catecholic Imidazolium and the Spin-Coated Films of Ionic Liquids, *Langmuir*, 2011, **27**(18), 11324–31.

77 O. Werzer, *et al.*, Ionic Liquid Nanotribology: Mica–Silica Interactions in Ethylammonium Nitrate, *Phys. Chem. Chem. Phys.*, 2012, DOI: 10.1039/C1CP23134K.

78 H. Yoshizawa, *et al.*, Fundamental mechanisms of interfacial friction. 1. Relation between adhesion and friction, *J. Phys. Chem.*, 1993, **97**(16), 4128–40.

79 K. Ueno, *et al.*, From Colloidal Stability in Ionic Liquids to Advanced Soft Materials Using Unique Media, *Langmuir*, 2011, **27**(15), 9105–15.

80 J. Dupont, *et al.*, On the structural and surface properties of transition-metal nanoparticles in ionic liquids, *Chem. Soc. Rev.*, 2010, **39**(5), 1780–804.

81 B. Wang, *et al.*, Ionic liquid-based stable nanofluids containing gold nanoparticles, *J. Colloid Interface Sci.*, 2011, **362**(1), 5–14.

82 D. Astruc, *et al.*, Nanoparticles as Recyclable Catalysts: The Frontier between Homogeneous and Heterogeneous Catalysis, *Angew. Chem., Int. Ed.*, 2005, **44**(48), 7852–72.

83 M. A. Gelesky, *et al.*, Laser-Induced Fragmentation of Transition Metal Nanoparticles in Ionic Liquids, *J. Am. Chem. Soc.*, 2005, **127**(13), 4588–9.

84 K. Ueno, *et al.*, Nanocomposite Ion Gels Based on Silica Nanoparticles and an Ionic Liquid: Ionic Transport, Viscoelastic Properties, and Microstructure, *J. Phys. Chem. B*, 2008, **112**(30), 9013–9.

85 K. Ueno, *et al.*, Soft Glassy Colloidal Arrays in an Ionic Liquid: Colloidal Glass Transition, Ionic Transport, and Structural Color in Relation to Microstructure, *J. Phys. Chem. B*, 2010, **114**(41), 13095–103.

86 P. Wang, *et al.*, Gelation of Ionic Liquid-Based Electrolytes with Silica Nanoparticles for Quasi-Solid-State Dye-Sensitized Solar Cells, *J. Am. Chem. Soc.*, 2003, **125**(5), 1166–7.

87 T. Nakashima, *et al.*, Quantum dots-ionic liquid hybrids: efficient extraction of cationic CdTe nanocrystals into an ionic liquid, *Chem. Commun.*, 2005, (12), 1643–5.

88 D. F. Evans, *et al.*, *The Colloidal Domain*, Wiley, New York, 2nd edn, 1999.

89 R. Pashley, Hydration forces between mica surfaces in electrolyte solutions, *Adv. Colloid Interface Sci.*, 1982, **16**, 57–62.

90 S. Perkin, *et al.*, Dynamic properties of confined hydration layers, *Faraday Discuss.*, 2009, **141**, 399–413.

91 R. Goldberg, *et al.*, Breakdown of hydration repulsion between charged surfaces in aqueous Cs + solution, *Phys. Chem. Chem. Phys.*, 2008, **10**, 4939–45.

92 A. A. H. Padua, *et al.*, Molecular Solutes in Ionic Liquids: A Structural Perspective, *Acc. Chem. Res.*, 2007, **40**(11), 1087–96.

93 A. S. Pensado, *et al.*, Solvation and Stabilization of Metallic Nanoparticles in Ionic Liquids, *Angew. Chem., Int. Ed.*, 2011, **50**(37), 8683–7.